FEBS Letters 555 (2003) 274–278 FEBS 27852

Functional consequences of an in vivo mutation in exon 10 of the human GLUT1 gene

Peter Lange[a], Elena Gertsen[b], Ingrid Monden[a], Jörg Klepper[b], Konrad Keller[a,*]

[a] *Institute of Pharmacology, Freie Universität Berlin, Thielallee 67–73, D-14195 Berlin, Germany*
[b] *Department of Pediatrics and Pediatric Neurology, University of Essen, Hufelandstr. 55, D-45122 Essen, Germany*

Received 16 September 2003; revised 23 October 2003; accepted 27 October 2003

First published online 5 November 2003

Edited by Judit Ovádi

Abstract The functional consequences of an in vivo heterozygous insertion mutation in the human facilitated glucose transporter isoform 1 (GLUT1) gene were investigated. The resulting frameshift in exon 10 changed the primary structure of the C-terminus from 42 in native GLUT1 to 61 amino acid residues in the mutant. Kinetic studies on a patient's erythrocytes were substantiated by expressing the mutant cDNA in *Xenopus laevis* oocytes. K_m and V_{max} values were clearly decreased explaining pathogenicity. Targeting to the plasma membrane was comparable between mutant and wild-type GLUT1. Transport inhibition by cytochalasin B was more effective in the mutant than in the wild-type transporter. The substrate specificity of GLUT1 remained unchanged.

Key words: Facilitated glucose transporter isoform 1; Facilitated glucose transporter isoform 1 deficiency syndrome; Transport kinetics; *Xenopus* oocyte

1. Introduction

GLUT1 deficiency syndrome (GLUT1-DS) is caused by various de novo mutations in the facilitated human glucose transporter 1 gene (1p35–31.3) [1,2]. Mutational analysis of GLUT1 (SLC2A1) revealed a great variety of mutation types such as silent mutations, missense mutations, nonsense mutations, deletion and insertion mutations, frameshift mutations, or splice site mutations. Prominent clinical symptoms are persistent hypoglycorrhachia, seizures, and developmental delay. Since these mutations are heterozygous the further characterization of functional consequences requires a valid heterologous expression system for the affected allele. Using the *Xenopus laevis* expression system, previous kinetic analysis of the G91D mutation in the highly conserved motif R-X-G-R-R within the second cytoplasmic loop [3], of the T310I mutation in transmembrane segment 8, and of the R126H mutation within the third extracellular loop [4] not only confirmed these mutations as pathogenic but also led to novel insights into structure–function relationship of GLUT1.

Out of 22 published human GLUT1 mutations only two nonsense mutations have been identified in exon 10 resulting in a stop codon and truncation of the carboxy-terminus that most likely abolishes glucose transport [2]. In parallel, patients with GLUT1-DS carrying insertion mutations appear to be more severely affected than those with missense mutations [1]. In this study, an insertion mutation with 14 additional base pairs in exon 10 inserted between nucleotide sequence 1540 and 1541 (numbering according to the GenBank M20681) was identified in a 5 year old girl with GLUT1-DS. Due to the resulting frameshift the mutant gene encodes a GLUT1 protein with a cytoplasmic C-terminal domain containing 61 instead of the 42 native amino acid residues. Following the first three N-terminal amino acid residues of the C-terminus, the primary structure of this domain is different in sequence from wild-type GLUT1. The functional role of the C-terminus was previously addressed in wild-type GLUT1 by deletion mutagenesis, point mutations, generation of chimeras between GLUT1 and different members of the GLUT family, and cloning of a C-terminal binding protein [5–11]. From these studies it became obvious that the C-terminus of GLUT1 is a functionally important structural element. Here we report for the first time how an in vivo insertion mutation in the human GLUT1 gene changing primary structure and length of the C-terminus influences the functional characteristics of the GLUT1 glucose transporter.

2. Materials and methods

2.1. The patient and GLUT1 genomic analyses

This 5 year old girl presented with seizures and developmental delay in late infancy. A low glucose concentration in the cerebrospinal fluid was suggestive of impaired GLUT1-mediated glucose transport across the blood–brain barrier. DNA was isolated from white blood cells by standard protocols. Genomic DNA was used as a template for polymerase chain reaction with specific primers of the human GLUT1 gene as described previously [12]. Amplification products were visualized by ethidium bromide staining on agarose gels, purified, and subjected to forward (F) and reverse (R) sequencing by an automated DNA sequencer using the following primers at exon 10: (F) ATG ACT CCA ACC AAG TGT GTC; (R) TGT GCT CCT GAG AGA TCC TTA. Fourteen additional base pairs (TTCAAAG-TTCCTGA) are inserted between nucleotides 1540 and 1541 (numbering according to GenBank M20681, starting at position 180–182).

2.2. Zero-trans 3-O-methyl-D-glucose (3-OMG) entry into erythrocytes

The assay has been described in detail elsewhere [13]. Briefly, blood specimens were collected in citrate–dextrose–phosphate solution, immediately put on wet ice, and processed within 10 days. All procedures were performed at 4°C. Blood samples were washed three times in phosphate-buffered saline and aliquots were incubated with increas-

*Corresponding author. Fax: (49)-30-8445 1818.
E-mail address: kellerfu@zedat.fu-berlin.de (K. Keller).

Abbreviations: 2-DOG, 2-deoxy-D-glucose; GLUT1, facilitated glucose transporter isoform 1; GLUT1-DS, Glut1 deficiency syndrome; 3-OMG, 3-*O*-methyl-D-glucose

0014-5793/03/$22.00
doi:10.1016/S0014-5793(03)01247-X

ing concentrations of ^{14}C-labeled 3-OMG. Uptake was terminated after 15 s, the aliquots were washed twice, lysed, bleached, and counted in a scintillation counter (Tricarb 2300, Canberra Packard, Germany).

2.3. Mutagenesis, in vitro transcription, and expression in X. laevis oocytes

The above indicated insertion mutation identified in the patient was generated in the pSP64T-GLUT1 plasmid [14–16] using the QuickChange® site-directed mutagenesis kit (Stratagene Europe, Amsterdam, The Netherlands). The correct mutagenesis was confirmed by automated DNA sequence analysis. The *Xba*I-linearized plasmid served as template to transcribe mutant and wild-type cRNAs using the in vitro transcription protocol provided by Ambion (mMESSAGE mMACHINE, Ambion, Austin, TX, USA). The amount of transcribed cRNA was calculated by counting the radioactivity of incorporated [^{35}S]thio-UTP. The integrity of cRNA was checked on a gel. For each preparation, the concentrations of cRNAs were adjusted to values of ~0.3 mg/ml. Fifty nanoliters of cRNA was injected into *Xenopus* oocytes which 24 h earlier had been manually isolated from ovarian lobes. Details of collection, defolliculation, and culture of *Xenopus* oocytes as well as cRNA microinjection have been described previously [17]. According to the induced frameshift the mutant cRNA translates into a mutant GLUT1 protein whose C-terminus contains 61 instead of 42 amino acid residues. Except for the first three N-terminal residues of the C-terminus the primary sequence is different between mutant and wild-type GLUT1: wild-type: ^{451}**KVP**-E-T-K-G-R-T-F-D-E-I-A-S-G-F-R-Q-G-G-A-S-Q-S-D-K-T-P-E-E-L-F-H-P-L-G-A-D-S-Q-V^{492}; mutant: ^{451}**KVP**-D-S-K-F-L-R-L-K-A-G-P-S-M-R-S-L-P-A-S-G-R-G-E-P-A-K-V-I-R-H-P-R-S-C-S-I-P-W-G-L-I-P-K-C-E-S-P-Q-I-T-S-P-A-C-S-Q-Q-P^{511}.

2.4. Kinetic analysis and inhibition by cytochalasin B

Kinetic analysis was assessed under zero-trans and equilibrium exchange conditions. Zero-trans entry was determined using tritium-labeled 2-deoxy-D-glucose (2-DOG, 2 μCi/0.5 ml transport assay, 30 min uptake time period, 10–15 oocytes per assay) according to a standard protocol [17]. 2-DOG concentrations ranged from 50 μM (standard assay) up to 25 mM (for Michaelis–Menten kinetics). Under equilibrium exchange condition (details in [17]) *Xenopus* oocytes were equilibrated with five 3-OMG concentrations (2, 10, 30, 50, and 100 mM) for 12 h. After addition of tritium-labeled 3-OMG (5 μCi/0.5 ml assay) accumulation of radioactivity in *Xenopus* oocytes was measured at seven time points (after 2, 5, 10, 20, 30, 40, and 50 min). Accumulation curves were linearized by logarithmic transformation and the negative reciprocals of the slopes plotted against equilibrium substrate concentrations (Hanes plot). All results were corrected for uptake in water-injected *Xenopus* oocytes.

Inhibition of 2-DOG uptake by cytochalasin B was determined at 0.1, 0.5, 1.0, 5.0, and 10.0 μM inhibitor concentrations. The mean fractional uptake rates (inhibited/non-inhibited 2-DOG uptake) were calculated after subtraction of values from water-injected *Xenopus* oocytes.

GraphPad Prism® software was used for calculation of K_m and V_{max} values.

2.5. Confocal laser scanning microscopy and Western dot blot analysis

Immunocytochemistry was performed as described previously [16] with the following modifications: the first antibody used was raised against the whole GLUT1 protein (a kind gift from Dr. A. Schürmann, DifE, Berlin, Germany), and fixed oocytes were frozen before cutting them into halves with a standard freezing microtome. In the line scan mode, fluorescence was scanned through a depth of 10 μm along a line drawn from outside the plasma membrane up to 50 μm into the cell interior.

Plasma membrane fractions were prepared according to the procedure of Keller et al. [17] with a slight modification [18]. Western dot blots were performed as described previously [19,20] using the chemiluminescent detection kit for horseradish peroxidase (Applichem, Darmstadt, Germany). The first antibody (see above) was used at 1:700 dilution; the anti-rabbit IgG (whole molecule) peroxidase-conjugated second antibody, developed in goat (Sigma, St. Louis, MO, USA), was diluted 1:1000. Five, 10, 25, and 50 ng of purified GLUT1 (a kind gift from Dr. G. Lienhard, Hanover, NH, USA) served as standards for the comparison of signal intensities.

2.6. Materials

The HPLC-purified oligonucleotides were obtained from Sigma (Taufkirchen, Germany). The radiolabeled glucose analogs 2-[1,2-^{3}H]deoxy-D-glucose (concentration 37 MBq/ml, specific activity 876.9 GBq/mmol) and 3-*O*-[methyl-^{3}H]D-glucose (concentration 37 MBq/ml, specific activity 2.3 TBq/mmol) were purchased from Perkin Elmer Life Science (Boston, MA, USA). 2-DOG, 3-OMG, and collagenase type I were from Sigma. Female *X. laevis* frogs were from African Xenopus Facility C.C. (Knysna, Republic of South Africa).

3. Results

The insertion of 14 additional nucleotides in exon 10 of the human glucose transporter GLUT1 gene led to changes in the amino acid sequence and the length of the C-terminal domain (see Section 2). Functional consequences were suggested after detection of a low glucose concentration in the cerebrospinal fluid. Fig. 1 presents the results of mutant GLUT1-mediated zero-trans entry of 3-OMG into erythrocytes. Because only one allele is affected this study represents a mixed population of normal and mutated red blood cells. Both the half saturation constant and V_{max} of mutant GLUT1 were lowered to about 30% of that of control erythrocytes. Following in vitro mutagenesis the cDNA was subcloned into the expression vector pSP64T, transcribed into mutant cRNA, injected into *Xenopus* oocytes, and translated into the mutant GLUT1. Fig. 2 confirms the results from the patient's erythrocytes demonstrating that the heterologously expressed mutant GLUT1 transports 2-DOG at rates that were only 15% of that of wild-type GLUT1. Confocal laser microscopy allowed a rough comparison between fluorescence intensities of the mutant and wild-type GLUT1 proteins that were recorded from oocyte halves at the plasma membrane area and adjacent portions of the cytoplasm (Fig. 3A). In the line plot mode (Fig. 3B), semi-quantitative analyses of fluorescence intensities (details in Section 2) support the notion that the levels of expression in the plasma membrane are comparable between mutant and wild-type GLUT1. In the Western dot blot of plasma membrane fractions, the signal of the mutant GLUT1 appears marginally less intense than that of wild-type GLUT1 (Fig. 3C). We conclude from Fig. 3 that neither translation of the mutant cRNA nor targeting of the mutant transporter to the plasma membrane is changed to an extent

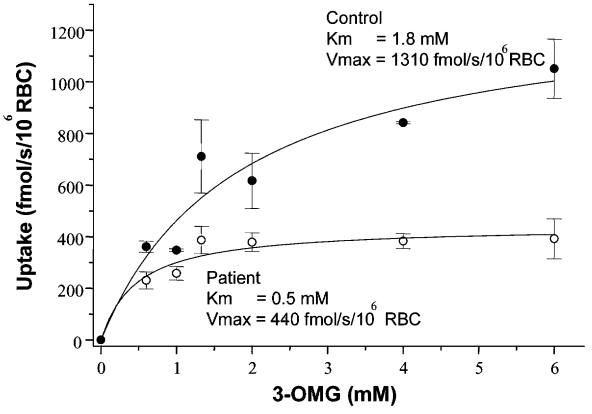

Fig. 1. Zero-trans entry of 3-OMG into erythrocytes of the patient (○) and two intra-assay controls (●, means ± S.E.M.) as velocity in fmol/s/10^6 RBC vs. substrate concentration in mmol/l, four determinations/data point.

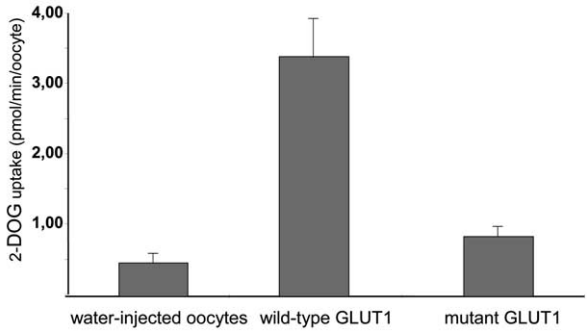

Fig. 2. 2-DOG uptake rates. Uptake was determined at 50 μmol/l tritium-labeled 2-DOG for 30 min in water-injected *Xenopus* oocytes and oocytes expressing wild-type GLUT1 or the GLUT1 C-terminal mutant (mean ± S.D.). Each assay included 30 *Xenopus* oocytes per group.

that could explain the dramatically reduced transport activity of this mutant GLUT1.

In order to further analyze the functional characteristics of the mutant we investigated the kinetics under two conditions, i.e. zero-trans entry using 2-DOG and equilibrium exchange entry using 3-OMG as glucose analogs. Representative plots are presented in Fig. 4. In keeping with the data obtained from erythrocytes (Fig. 1) both the apparent half-saturation rate constant and the maximal velocity of zero-trans 2-DOG uptake were decreased by the aberration (Fig. 4A). The kinetic data for wild-type GLUT1 are in agreement with published results [21,22]. As shown in Fig. 4B, lowering of the half-saturation rate constant by the mutation was confirmed in the equilibrium exchange experiment that uses 3-OMG as a glucose analog. Unlike 2-DOG, 3-OMG is transported but not phosphorylated upon entry into the cell. Because of the extremely low catalytic activity of the mutant, accumulation of radioactivity at 100 mM 3-OMG equilibrium concentration was not significantly different from background (missing value in the Hanes plot). The K_m of wild-type GLUT1, in line with previously published apparent Michaelis constants [17,21,23], confirms the difference between values determined under equilibrium exchange and zero-trans entry condition, respectively. Because of the extensive scale of the equilibrium exchange experiments different batches of oocytes from the same animal had to be used for the kinetics of wild-type and mutant GLUT1. *Xenopus* oocytes from different batches may express slightly different levels of transporter protein in the plasma membrane, so that values for V_{max} are not mentioned for comparison in Fig. 4B.

Mutant and wild-type GLUT1-expressing *Xenopus* oocytes were subjected to transport inhibition by the exofacial inhibitor ethylidene glucose and the endofacial inhibitor cytochalasin B. Whereas the structural changes of the C-terminus did not affect the inhibition of 2-DOG (50 μmol/l) uptake by ethylidene glucose (tested at the concentrations of 2, 5, 10, 20, 50, and 100 mmol/l; data not shown), cytochalasin B was more effective in the mutant transporter compared with control (Fig. 5). Substrate specificity was also tested on the basis of 2-DOG uptake modification by L-glucose, D-mannose, D-galactose, and D-fructose, each at 100 mM concentration. Competition of these hexoses with 2-DOG (50 μmol/l) for transport was the same in mutant and wild-type GLUT1 (data not shown).

4. Discussion

An in vivo insertion mutation in the human GLUT1 gene (1p35–31.3) led to an alteration in the C-terminus of the transport protein. This changed GLUT1 toward a higher affinity

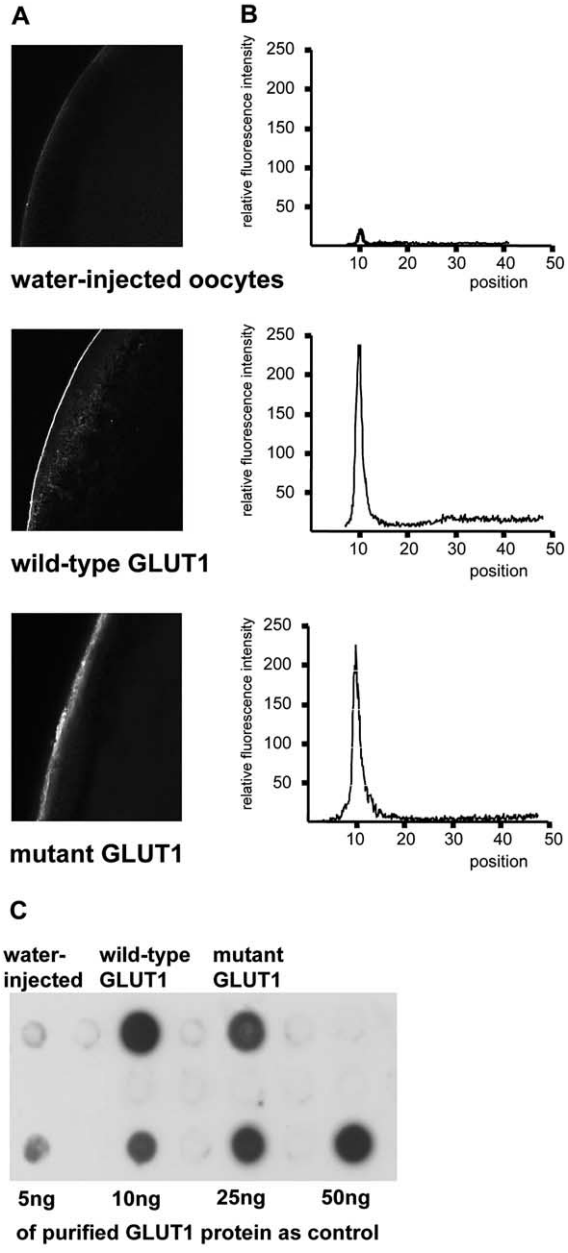

Fig. 3. Confocal laser microscopy was performed in cut oocyte halves of three randomly selected *Xenopus* oocytes using a first antibody raised against the whole GLUT1 protein (a kind gift from Dr. A. Schürmann) followed by a second FITC-conjugated goat anti-rabbit IgG antibody. Representative images (A) and line plots (B) were obtained by scanning the fluorescence through a depth of 10 μm along a line of about 50 μm drawn from the outer plasma membrane into the cell interior. The *x*-axis of line plots indicates the distance in μm, the *y*-axis represents the relative fluorescence intensities in arbitrary units. C: For Western dot blot the same first antibody as above was used at a 1:700 dilution. The anti-rabbit IgG peroxidase-conjugated second antibody (Sigma) was used at a 1:1000 dilution. Five, 10, 25, and 50 ng of purified GLUT1 (a kind gift from Dr. G. Lienhard) were applied as standards.

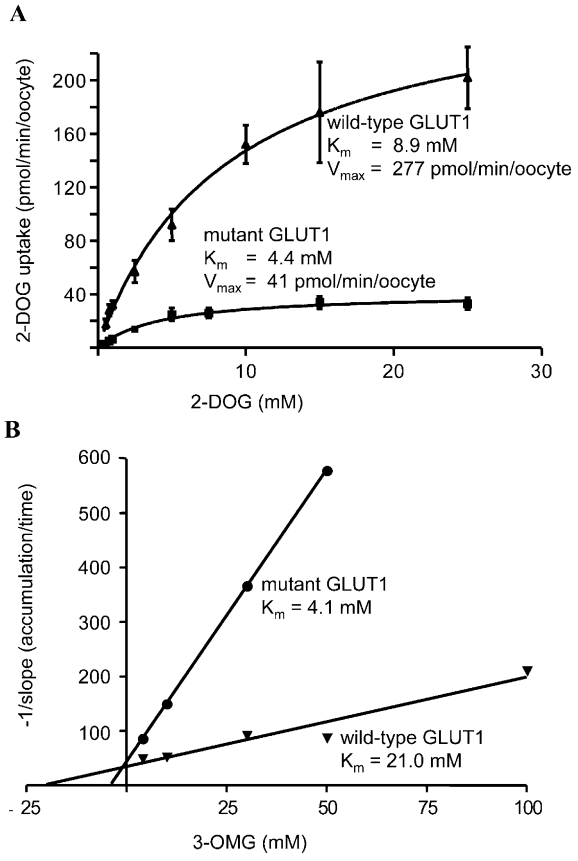

Fig. 4. Kinetic analysis. A: Zero-trans entry of 2-DOG at the indicated concentrations was determined in *Xenopus* oocytes expressing wild-type GLUT1 or the GLUT1 C-terminal mutant (Michaelis–Menten graphs). Each value is derived from the mean of data from 15–30 oocytes (mean ± S.D.) and is corrected for uptake in water-injected *Xenopus* oocytes. B: Equilibrium exchange entry kinetics were performed at the indicated 3-OMG equilibrium concentrations. Accumulation of [^{3}H]3-OMG was assessed at 2, 5, 10, 20, 30, 40, and 50 min and linearized by logarithmic transformation. For each time point, 8–10 *Xenopus* oocytes per group were included in the assay. Values from water-injected oocytes were always subtracted. In the mutant, accumulation of radioactivity at 100 mM 3-OMG equilibrium concentration led to negligible counts. The negative reciprocals of the slopes were plotted against 3-OMG concentrations (Hanes plots). K_m and V_{max} values were calculated using the GraphPad Prism® software.

and lower capacity. The functional role of the C-terminal domain of GLUT1 has been addressed by several scientific groups with partly contradictory results. A deletion of the entire C-terminus abolishes the catalytic activity of GLUT1 [5]. A loss of 24 residues at the C-terminal end does not interfere with GLUT1 function while a greater deletion markedly reduced transport activity [6]. Point mutations G466→E and F467→L do not significantly alter 2-DOG uptake, whereas the substitution of R468 with leucine leads to a slight lowering of K_m [6]. Studies with various chimeric constructs containing parts of GLUT1 and GLUT4 underline the importance of the GLUT1 C-terminus with regard to the exocytosis rate from the endosomal compartment to the cell surface [8]. In a GLUT1/GLUT2 chimera, the K_m value was intermediate between those of the two isoforms [10]. Results from a GLUT1/GLUT5 chimera, however, support the notion that the C-terminal domain does not determine isoform-specific targeting [9]. Regarding relevant isoform-specific sequences within the C-terminus, motifs like ^{489}L-L^{490} or ^{498}T-E-L-E-Y-L-G-P^{505} in GLUT4 are not expressed in the mutant GLUT1 C-terminus. The ^{463}I-A-S-G-F-R^{468} sequence within the GLUT1 C-terminal domain, shown to function as an amplifier for glucose signaling to extracellular signal-regulated kinase [24], is missing in the mutant C-terminus.

To our knowledge a single publication refers to functional consequences of an enlargement of the C-terminal domain of GLUT1. The group of May and coworkers changed the C-terminus by adding 31 residues from the connecting peptide of proinsulin to the C-terminal end of GLUT1 without modifying GLUT1 catalytic activity [25]. Therefore, the enlargement per se seems not to be an important determinant for the extremely low catalytic activity of this in vivo mutation. The highly conserved motif ^{501}K-V-P-E-T^{555} at the N-terminal end is changed in the mutant to the homologous sequence ^{501}K-V-P-D-S^{555}. We do not know the implication of a glutamate to aspartate or threonine to serine substitution in GLUT1 transport activity. Notably, the mutation dramatically changed the balance between positively and negatively charged amino acid residues within the C-terminus (wild-type and mutant amino acid sequences in Section 2). Only 5% of the side chains were negatively charged in the mutant transporter compared with 17% in native GLUT1, whereas the number of positively charged amino acids increased from five to 10 residues in the mutant. Acidic amino acids in the C-terminus of wild-type GLUT1 may form electrostatic bonds with basic residues in cytoplasmic loops (e.g. in the R-X-G-R-R motif) stabilizing the helical packing arrangement. This interaction may be partly disrupted by the in vivo mutation leading to negative functional consequences. We have no explanation concerning the more effective inhibition by cytochalasin B of 2-DOG uptake mediated by the mutant transporter compared with inhibition in wild-type GLUT1.

In conclusion, our results identified the pathogenic mechanism of an insertion mutation in a patient with GLUT1-DS. The resulting frameshift leading to elongation and change in the primary structure of the GLUT1 C-terminus impairs GLUT1 function but not or only marginally GLUT1 expression or translocation to the cell surface. In line with previous

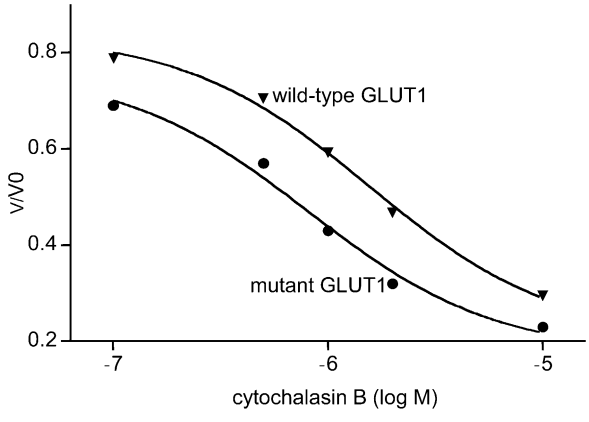

Fig. 5. Inhibition by cytochalasin B (CB) of 2-DOG uptake. *Xenopus* oocytes expressing wild-type GLUT1 or the C-terminal mutant were incubated with CB at the indicated concentrations. Values obtained in water-injected *Xenopus* oocytes were always subtracted. Inhibition is expressed as mean fractional uptake rates (v/v_o = inhibited/non-inhibited uptake rates). Curve fitting was performed with the GraphPad Prism® software.

observations, the C-terminus is essential for GLUT1 transport function. Further analyses of GLUT1 mutations in patients with GLUT1-DS will help to identify additional structure–function relationships within the GLUT1 transport protein.

Acknowledgements: P.L. was supported by Research Grant Ke 390/6-2 from the Deutsche Forschungsgemeinschaft.

References

[1] De Vivo, D.C., Leary, L. and Wang, D. (2002) J. Child Neurol. 17, 15–25.
[2] Klepper, J. and Voit, T. (2002) Eur. J. Pediatr. 161, 295–304.
[3] Klepper, J., Monden, I., Guertsen, E., Voit, T., Willemsen, M. and Keller, K. (2001) FEBS Lett. 489, 104–109.
[4] Brockmann, K., Wang, D., Korenke, C.G., von Moers, A., Ho, Y.Y., Pascual, J.M., Kuang, K., Yang, H., Ma, L., Kranz-Eble, P., Fischbarg, J., Hanefeld, F. and De Vivo, D.C. (2001) Ann. Neurol. 50, 476–485.
[5] Oka, Y., Asano, T., Shibasaki, Y., Lin, J.L., Tsukuda, K., Katagiri, H., Akanuma, Y. and Takaku, F. (1990) Nature 345, 550–553.
[6] Muraoka, A., Hashiramoto, M., Clark, A.E., Edwards, L.C., Sakura, H., Kadowaki, T., Holman, G.D. and Kasuga, M. (1995) Biochem. J. 311, 699–704.
[7] Dauterive, R., Laroux, S., Bunn, R.C., Chaisson, A., Sanson, T. and Reed, B.C. (1996) J. Biol. Chem. 271, 11414–11421.
[8] Yeh, J.I., Verhey, K.J. and Birnbaum, M.J. (1995) Biochemistry 34, 15523–15531.
[9] Inukai, K., Takata, K., Asano, T., Katagiri, H., Ishihara, H., Nakazaki, M., Fukushima, Y., Yazaki, Y., Kikuchi, M. and Oka, Y. (1997) Mol. Endocrinol. 11, 442–449.
[10] Noel, L.E. and Newgard, C.B. (1997) Biochemistry 36, 5465–5475.
[11] Bunn, R.C., Jensen, M.A. and Reed, B.C. (1999) Mol. Biol. Cell 10, 819–832.
[12] Klepper, J., Wang, D., Fischbarg, J., Vera, J.C., Jarjour, I.T., O'Driscoll, K. and De Vivo, D.C. (1999) Neurochem. Res. 24, 587–594.
[13] Klepper, J., Garcia-Alvarez, M., Wang, D., O'Driscoll, K. and De Vivo, D.C. (1999) J. Clin. Lab. Anal. 13, 116–121.
[14] Krieg, P.A. and Melton, D.A. (1984) Nucleic Acids Res. 14, 7057–7070.
[15] Mueckler, M. and Lodish, H.F. (1986) Cell 44, 629–637.
[16] Olsowski, A., Monden, I., Krause, G. and Keller, K. (2000) Biochemistry 39, 2469–2474.
[17] Keller, K., Strube, M. and Mueckler, M. (1989) J. Biol. Chem. 264, 18884–18889.
[18] Garcia, J.C., Strube, M., Leingang, K., Keller, K. and Mueckler, M. (1992) J. Biol. Chem. 267, 7770–7776.
[19] Wellner, M., Monden, I., Mueckler, M. and Keller, K. (1995) Eur. J. Biochem. 227, 454–458.
[20] Monden, I., Olsowski, A., Krause, G. and Keller, K. (2001) Biol. Chem. 382, 1551–1558.
[21] Bell, G.I., Burant, C.F., Takeda, J. and Gould, G.W. (1993) J. Biol. Chem. 268, 19161–19164.
[22] Keller, K. and Olsowski, A. (1999) Recent Res. Dev. Biochem. 1, 29–44.
[23] Nishimura, H., Pallardo, F.V., Seidner, G.A., Vannuci, S., Simpsin, I.A. and Birnbaum, M.J. (1993) J. Biol. Chem. 268, 8514–8520.
[24] Bandyopadhyay, G., Sajan, M.P., Kanoh, Y., Standaert, M.L., Burke Jr., T.R., Quon, M.J., Reed, B.C., Dikic, I., Noel, L.E., Newgard, C.B. and Farese, R. (2000) J. Biol. Chem. 275, 40817–40826.
[25] Due, A.D., Zhi-chao, Q., Thomas, J.M., Buchs, A., Powers, A.C. and May, J.M. (1995) Biochemistry 34, 5462–5471.